



REVIEW

Flow Regimes in Bubble Columns with and without Internals: A Review

Ayat N. Mahmood¹, Amer A. Abdulrahman¹, Laith S. Sabri^{1,*}, Abbas J. Sultan¹, Hasan Shakir Majdi² and Muthanna H. Al-Dahhan³

¹Department of Chemical Engineering, University of Technology-Iraq, Baghdad, Iraq

²Chemical and Petroleum Industries Engineering Department, Al-Mustaqbal University College, Babylon, Iraq

³Department of Chemical and Biochemical Engineering, Missouri University of Science and Technology, Rolla, USA

*Corresponding Author: Laith S. Sabri. Email: lssf25@umsystem.edu

Received: 26 November 2022 Accepted: 20 February 2023 Published: 14 December 2023

ABSTRACT

Hydrodynamics characterization in terms of flow regime behavior is a crucial task to enhance the design of bubble column reactors and scaling up related methodologies. This review presents recent studies on the typical flow regimes established in bubble columns. Some effort is also provided to introduce relevant definitions pertaining to this field, namely, that of “void fraction” and related (local, chordal, cross-sectional and volumetric) variants. Experimental studies involving different parameters that affect design and operating conditions are also discussed in detail. In the second part of the review, the attention is shifted to cases with internals of various types (perforated plates, baffles, vibrating helical springs, mixers, and heat exchanger tubes) immersed in the bubble columns. It is shown that the presence of these elements has a limited influence on the global column hydrodynamics. However, they can make the homogeneous flow regime more stable in terms of transition gas velocity and transition holdup value. The last section is used to highlight gaps which have not been filled yet and future directions of investigation.

KEYWORDS

Hydrodynamics; flow regime; bubble column; heat-exchanging internals

1 Introduction

Bubble columns are reactors that are frequently employed in various industrial applications, such as wastewater treatment, absorption, fermentation, bioreactions, coal liquefaction, acetylene production, methylene synthesis, and Fisher-Tropsch synthesis [1]. A bubble column reactor is simply a cylindrical or square-shaped column with a gas sparger section located at its bottom. A gas phase is introduced into the liquid or liquid-fine solid catalyst medium through the sparger section. A reactor containing only liquid and gas reactants is called a bubble column. A reactor containing liquid and gas reactants and miniscule amounts of a catalyst is called a slurry bubble column. Bubble/slurry bubble column reactors operate in different modes, such as semi-batch, countercurrent, or co-current modes. Bubble columns offer many advantages, such as the absence of moving parts; good mixing; low energy requirements and construction and operating costs; and good mass and heat transfer. The efficiency and effectiveness of bubble columns increase with the addition of internals, baffles, or plates to reduce back mixing and dead zones [2].



This work is licensed under a Creative Commons Attribution 4.0 International License, which permits unrestricted use, distribution, and reproduction in any medium, provided the original work is properly cited.

Designing and selecting the appropriate spargers for bubble columns are crucial because these components determine bubble size, bubble rising, and flow regime distribution [3]. Many types of spargers, such as porous plates, perforated plates, spider-type spargers, single/multiple nozzles, and ring-type spargers, are used in bubble columns. Numerous experimental studies on the effect of spargers on hydrodynamics, which have essential effects on flow regime performance, have been performed by [4,5]. Lau et al. (2010) used three types of gas distributors, namely, single nozzles, perforated plates, and porous plates, to investigate the effect of static liquid height-to-column diameter (H/D_C) ratios of 2–7.2 and found that increasing the H/D_C ratio decreased the overall gas holdup (ϵ_G). However, this effect diminished at H/D_C ratios higher than 4 when bubbles reached their equilibrium size, which caused a minimal increase in the average ϵ_G . Many types of bubble columns exist they include simple bubble columns, cascade bubble columns with sieve trays, packed bubble columns, multishift bubble columns, bubble columns with static mixers, bubble columns with internals, bubble columns with jet reactors, fluidized bed reactors, and slurry reactors. In industrial settings, these reactors are employed as chemical reactors for a variety of activities [6] as shown in Fig. 1. The comparison between with and without internals Bubble columns as shown below:

Bubble columns with internals	Bubble columns without internals
High mass transfer.	Low mass transfer.
High heat transfer.	Lower heat transfer.
Better mixing characteristics.	High back mixing.
Low pressure drops.	Lower per pass conversion.
Simple construction.	Difficult to control of temperature.
No internal moving parts.	Difficult to model.
High liquid holds up.	low liquid holds up.

Typically, flow regimes are determined either through subjective evaluations or through objective evidence. The input parameters for flow regime maps based on physical mechanisms are determined by the superficial velocities of liquid and gas, which are typically not measurably during on-line operations. In laboratory investigations, flow visualization is typically used to make subjective judgments [7,8], void fraction fluctuation obtained by radiation technique [9] or impedance technique [10] and pressure fluctuation [11].

In laboratory investigations, subjective judgements are usually made by:

a-flow visualization by [12].

b-void fraction fluctuation obtained by radiation technique [9].

c-void fraction fluctuation obtained by impedance technique [13].

d-void fraction fluctuation obtained by pressure fluctuation [11].

If the flow is fast and the void fraction is high or if the pipe is opaque, flow visualization may not be particularly accurate or realized. A many-to-many mapping between flow patterns and pressure fluctuations may occur from the two-phase pressure fluctuation's dependency on so many different variables. Additionally, some challenges brought on by the existence of two-phase fluids are difficult to overcome, such as the possibility of gas being trapped in pressure sensor lines, as noted by Jones et al. in 1976 [14]. Measurements of the void fraction variation can be obtained using radiation absorption techniques like the X-ray and gamma-ray absorption methods.

However, it seems that impedance techniques, rather than radiation approaches, are a superior alternative to undertaking flow regime identification due to safety and financial reasons (even though the temperature effect still needs to be overcome). The immediate response from the impedance measurement also enables on-line characterization for the majority of practical applications.

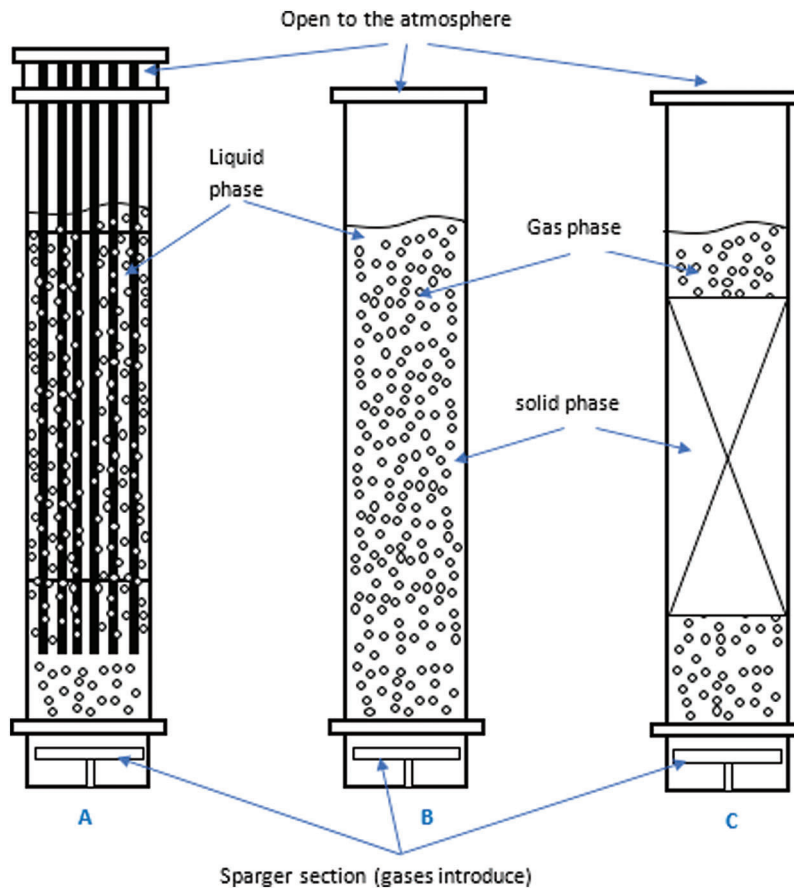


Figure 1: Three main three types of bubble columns: (A) bubble column with internals, (B) bubble/slurry bubble column, and (C) packed bed bubble column

In order to execute non-linear mapping from physical factors to flow regimes, statistical approaches and neural network systems have been used [15]. In this case, the neural network systems were more promising than the statistical approach. Previous neural network systems, on the other hand, needed to gather known input that is used for training as well as to undertake off-line benchmarking or cross-calibration.

2 Factors Affecting the Flow Regime

This section provides an explanation of the factors, such as mass transfer and bubble size distribution (BSD) and its forms, that affect flow regimes. Note that designs consider the exchange between gas in the form of air bubbles and liquid in the form of water. This assumption must be taken into account when altering gases or liquids in design calculations [8].

2.1 Fluid Dynamics

The fluid dynamics characteristics of bubble columns affect performance quality. For example, superficial gas velocity is the main factor affecting flow regimes in any multiphase system. Thus, two fundamental flow types are frequently seen to affect bubble column performance in most studies: homogeneous (bubbly flow) and heterogeneous (churn-turbulent flow) [16–18]. In homogeneous or bubbly flow, bubble size is uniformly distributed over the cross-sectional area of the column when superficial velocities are low and approximately less than 0.05 m/s [17]. Moreover, in homogeneous regimes, the parameter ε_G increases linearly with the increase in superficial gas velocity [19]. Therefore, at a certain gas velocity, the flow regime transitions from homogeneous to heterogeneous. Nonuniform bubble size and distribution and potential mixing are observed over the cross-sectional area of bubble columns at high superficial gas velocities approximately greater than 0.05 m/s. This regime is called the heterogeneous regime or churn-turbulent regime due to the high disturbance in the flow system inside the bubble column, as illustrated in Fig. 2. The homogeneous regime at low superficial gas velocities is also known as the bubble flow regime when the bubbles are small in size, spherical in shape, and rise in the vertical direction. • The transition regime: when the gas velocities increase compared to the bubble flow regime causes less stability in bubble behavior, and the bubble characterizes. • The heterogeneous regime at usually high superficial gas velocities is also defined as a churn turbulent regime due to the gas velocities that generate a parabolic radial profile, including the large bubbles. • The slug flow regime can be defined when the gas phase has very high superficial velocities in a small diameter of the reactors. Then, the bubble coalescence to be very large diameter slugs in the column.

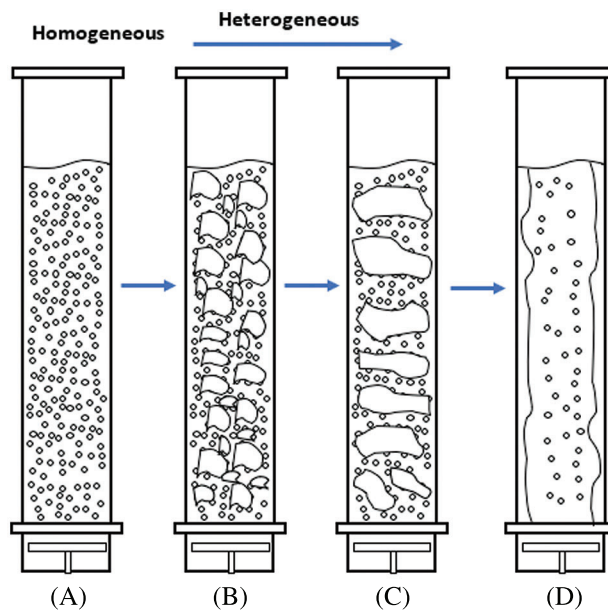


Figure 2: Types of flow regimes in multiphase flow systems in bubble columns. (A) Bubbly flow, (B) churn-turbulent flow, (C) sluggish flow, and (D) annular flow

2.2 Geometry and Operating Condition Mapping

Using flow maps to predict operational flow system information on the basis of the operating conditions and geometry of columns is important. These maps are used in many applications. For example, operational flow maps are utilized for large- and small-diameter two-phase flow systems [20]. Shah et al. established the best map that has been adopted as a design for bubble columns. The map for low-viscosity systems is applied

for all flow systems, whether homogeneous, transitional, or heterogeneous, because of its dependence on the diameter of the bubble column and the velocity of gas–liquid transfer perpendicular to the surface area as shown in Fig. 3. The gas holdup was measured for four zones under different initial bubble modes [6].

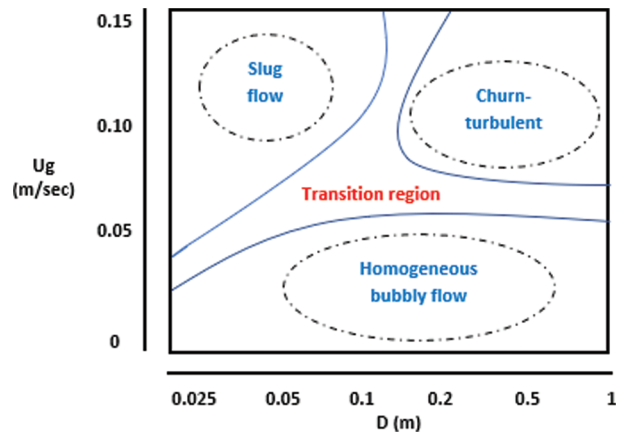


Figure 3: Schematic showing the different flow regimes based on operating conditions and column diameter [21]

2.3 Bubble Sizes and Shapes

Bubble sizes and shapes affect the flow regime behavior, and understanding and knowing these parameters are essential for bubble column design and performance. Current studies have demonstrated that the sizes, shapes, and distributions of bubbles exert a major effect on flow regimes due to their link to the bubble stability. Consequently, these parameters have a vital influence on hydrodynamics parameters, particularly ε_G distribution, inside bubble columns.

Along with ε_G , BSD provides an assessment of the interfacial area and is used in computational liquid dynamics (CFD) for model setup and validation. From a practical standpoint, BSD is a fundamental parameter of bubble column fluid dynamics. Its fluctuation is one of the primary causes of the effect of operational parameters on ε_G and the change in the flow regime. In addition to bubble forms, BSD (the aspect ratio) must be considered. Interface size and form are crucial for describing multiphase flows accurately.

2.4 Gas Holdup

ε_G is one of the main important dimensionless parameters characterizing the hydrodynamics of multiphase systems. It is defined as the volume fraction of gas in the total volume of the gas–liquid phases in bubble columns. ε_G depends on the period of time during which the gas remains inside the bubble column and the speed of its passage through the liquid [22]. The size of the reactor is affected by column design and operating conditions. Studies have shown that compared with the heterogeneous system, the homogeneous flow system is more prone to trapping gas because it is more sensitive to operating conditions [23,24].

$$\varepsilon_G = \frac{H_d - H_s}{H_d} \quad (1)$$

ε_G = gas hold up

H_d = hydrodynamic Hight

H_s = static Hight

$$\varepsilon_G = \frac{V_g}{v_g + v_l} \quad (2)$$

ε_G = gas hold up

V_g = volume of gas

v_l = volume of liquid

Using the traditional Bernoulli's law of energy conservation, we can calculate the void fraction.

$$\frac{1}{2} \rho v^2 + \rho gh + p = \text{constant} \quad (3)$$

where: $\frac{1}{2} \rho v^2$ is the Kinetic energy.

ρgh : potential energy

p : pressure.

$$\Delta p = \rho_m gh + F_F \quad (4)$$

F_F = fraction pressure.

$$\rho_m = (1 - \varepsilon_G) \rho_L + \varepsilon_G \rho_G \quad (5)$$

$$\varepsilon_G = \left(\frac{\rho_L}{\rho_L - \rho_G} \right) * \left(\frac{1 - \Delta P}{g \Delta h \rho_L} \right) \text{ Jia et al. [25].} \quad (6)$$

In a particular two-phase space, the void fraction is often expressed as the volume of vapor divided by the total volume of fluid. Rahim et al. [26] presented four generally used definitions of void fraction for various scenarios and measurement techniques: void fractions can be local, chordal, cross-sectional, and volumetric.

a-The local emptiness fraction is measured by using a tiny sensor to collect signals from a single spot.

b-The chordal void percent, which is employed in one-dimensional flows like intermittent (plug/slug) two-phase flow inside typically smaller channels, is defined as the length of the vapor over the entire length.

c-The percentage of cross-sectional area occupied by the vapor phase relative to the total cross-sectional area is known as the cross-sectional void fraction. Typically, optical or electrical techniques are used to measure this type of vacancy fraction.

d-The volumetric void fraction in a control volume is determined by dividing the volume of the vapor phase by the entire volume. By swiftly closing valves, one can determine the volumetric void fraction.

correlation ε_G

Many mathematical relations that are widely used to describe gas trapping (ε_G) have been studied previously as shown in [Table 1](#).

2.5 Gas/Liquid Velocity

Bubble columns can be operated in batch-wise, co-current, or countercurrent mode at $U_L = 0.01$ m/s. Various researchers have shown that normally, low liquid velocities have no effect on ε_G because bubble acceleration due to no stagnant operation is minimal if U_L is less than the bubble rise velocity [20].

Table 1: Mathematical correlations for ϵ_G distribution

Correlation	Condition	Ref.
$\epsilon_g = \frac{1}{\left[2 + \left(\frac{0.35}{U_g} \right) * \left\{ \frac{\rho l \sigma}{72} \right\}^{\frac{1}{3}} \right]}$	Atmospheric pressure and temperature.	Hughmark [27] For configuration (open tup configuration) both low & high air superficial velocities ($U_G = 0.004-0.45$ m/s)
$\epsilon_g = U_g / (0.3 + 2 U_g)$	Atmospheric pressure and temperature °C.	Mashelkar et al. [28] For AG configuration (annular gap configuration). ($U_G = 0.1-0.30$ m/s)
$\frac{\epsilon_g}{(1 - \epsilon_g)^4} = c_1 * \left(\frac{g d_c^2 \rho_l}{\sigma} \right)^{1/8} * \left(\frac{g d_c^3}{v_l^2} \right)^{1/2} * \frac{U_g}{\sqrt{g d_c}}$	Atmospheric pressure. $T = 25^\circ\text{C}$	Akita et al. [29]
$\epsilon_g = 0.505 U_g^{0.47} * \left(\frac{72}{\sigma} \right)^{2/3} * \left(\frac{1}{\mu_L} \right)^{0.05}$	Atmospheric pressure. $T = (16-20)^\circ\text{C}$	Hikitia et al. [30] $U_G = (0.00812-0.0565$ m/s)
$\frac{\epsilon_g}{(1 - \epsilon_g)^4} = 0.32 * \left(\frac{g d_c^2 \rho_l}{\sigma} \right)^{0.121} * \left(\frac{g d_c^3}{v_l^2} \right)^{0.86} * \frac{U_g}{\sqrt{g d_c}} * \left(\frac{\rho_g}{\rho_l} \right)^{0.068}$	Pressure 10 N/cm ² $T = 25^\circ\text{C}$.	Taitel et al. [7]
$\epsilon_g = 296 U_g^{0.44} \rho_L^{-0.98} \sigma^{-0.16} \rho_g^{0.19} \rho + 0.009$	Pressure plus one-half the total experimental hydrostatic pressure head.	O'Reilly et al. [31]
$\frac{\epsilon_g}{(1 - \epsilon_g)^n} = k_1 * C_a^{k_3} \ln \frac{\epsilon_g}{(1 - \epsilon_g)^n} = k_3 \ln (C_a) + \ln (k^*_1)$	Atmospheric pressure. $T = 25^\circ\text{C}$	Besagni et al. [32,33]
$\epsilon_g = 0.048 U_g^{0.720} d_p^{0.168} D_c^{0.125}$	Atmospheric pressure. $T = 25^\circ\text{C}$	Begovich et al. [34]
$\epsilon_g = 0.066 \left[\frac{U_L}{U_L + U_s} \right]^{-0.424}$	A three-phase bed under conditions simulating industrial units as closely as possible.	Catros et al. [35]
$\epsilon_g = 0.048 Fr_{g,dh}^{0.315} Fr_{L,dh}^{-0.098} M_o^{0.02} (1 + 34.09 d_p/d_h)^{-0.346}$	High operating temperatures (450°C) and pressures (17000 kPa).	Fan et al. [36]

(Continued)

Table 1 (continued)		
Correlation	Condition	Ref.
For dispersed large bubble regime $= 1.81Fr_g^{0.222}Re_L^{0.432}M_o^{0.02}$ for transition regime: $\varepsilon_g = 0.654Fr_g^{0.358}Re_L^{0.051}M_o^{0.02}$ for dispersed small bubble regime: $\varepsilon_g = 2.61Fr_g^{0.21}Re_L^{-0.372}M_o^{0.02}$	Atmospheric pressure. $T = 25^\circ C$	Song et al. [37]
• Middle and high gas holdup regions: $\varepsilon_g = 0.814Fr_g^{0.3987}Re_L^{-0.0977}$	Atmospheric pressure. $T = 25^\circ C$	Gorowara et al. [38]
$\varepsilon_g = 0.0139Re_g^{0.426}$	At atmospheric pressure and atmospheric temperature.	Safoniuk et al. [39]
$\varepsilon_g = 0.11Fr_g^{0.35}Re_L^{0.2}M_o^{0.075}Ar_1^{0.11}$	Atmospheric pressure. $T = 25^\circ C$	Ramesh et al. [40]
$\varepsilon_g = 0.4008Fr_g^{0.38547}Re_L^{-0.6712}$	Atmospheric pressure. $T = 24^\circ C$	Kumar et al. [41]
$\varepsilon_g = \varepsilon \left[\frac{U_g - U_{gl}}{U_g - U_l} \right]$	Atmospheric pressure. $T = 25^\circ C$	Nacef et al. [42]
$\varepsilon_g = 0.0023Re_g^{0.73}$	Atmospheric pressure. $T = 25^\circ C$	Jena et al. [43]
$\varepsilon_g = 0.015 U_g^{0.98}$	Atmospheric pressure. $T = 25^\circ C$	Abdel-Aziz et al. [44]
$\varepsilon_g = 0.256 Fr_g^{0.081} Re_L^{0.067} \left(\frac{P}{D_c} \right)^{0.79} (d_p/D_c)^{0.85}$	Atmospheric pressure. $T = 25^\circ C$	Rohini Kumar et al. [45]

Numerous authors have studied the properties of liquids in gas retention and mass transfer. They identified the liquid characteristics in terms of gas retention and mass transfer within the bubble column and discovered that liquid velocity in the presence of an opposite current has a strong actual effect on gas retention as represented by ε_G [46]. Therefore, gas retention increases and the value of ε_G is high if the current is opposite to the direction of the liquid, whereas ε_G is low if the current is in the direction of the liquid when velocities above 0.04 m/s are neglected [47]. Baawain et al. studied the relationship between mass transfer and bubble size and its effect on gas retention within a column in the presence of a current opposite to the liquid. They found that 5% of the weight of the gas and 1% of the bubble volume were retained due to the increase in the speed of bubbles but not in bubble size [48].

2.6 Bubble Column Configurations

Bubble column configurations are the main criteria that must be considered in the design of multiphase flow systems also there are important parameters such as Column size, Aspect ratio Gas sparger as shown in Fig. 4. Numerous studies have proven that large bubble column diameters (d_c) result in high reductions in ε_G . Moreover, bubble size and movement are influenced by the column wall. Besagni et al. [49] studied the relationship between d_c and ε_G and found that ε_G decreased with the increase in d_c and that viscous fluids

can be used when d_c was 0.15–0.23 m [50]. Behkish et al. [51] demonstrated the relationship between d_c and highly viscous fluids and proved that increasing d_c increased the viscosity of fluids that can be used there are also two parameter effected in design of bubble column.

A-Aspect ratio

The ratio of the initial liquid height to the column diameter (H/D) is defined as aspect ratio. Zhany et al. [52] studied the values of ε_G with liquid movements in homogenous flow systems and demonstrated that ε_G decreased as the bubble column size was reduced. Bubble sizes larger than the size needed for equilibrium reduced the efficiency of integration between the liquid and gas phases. The aspect ratio up to critical has turned to decrease the gas hold up and destabilize the homogeneous flow regime. Aspect ratio decreases the transition velocity; however, it alone is not sufficient to provide reliable information on flow regime stability.

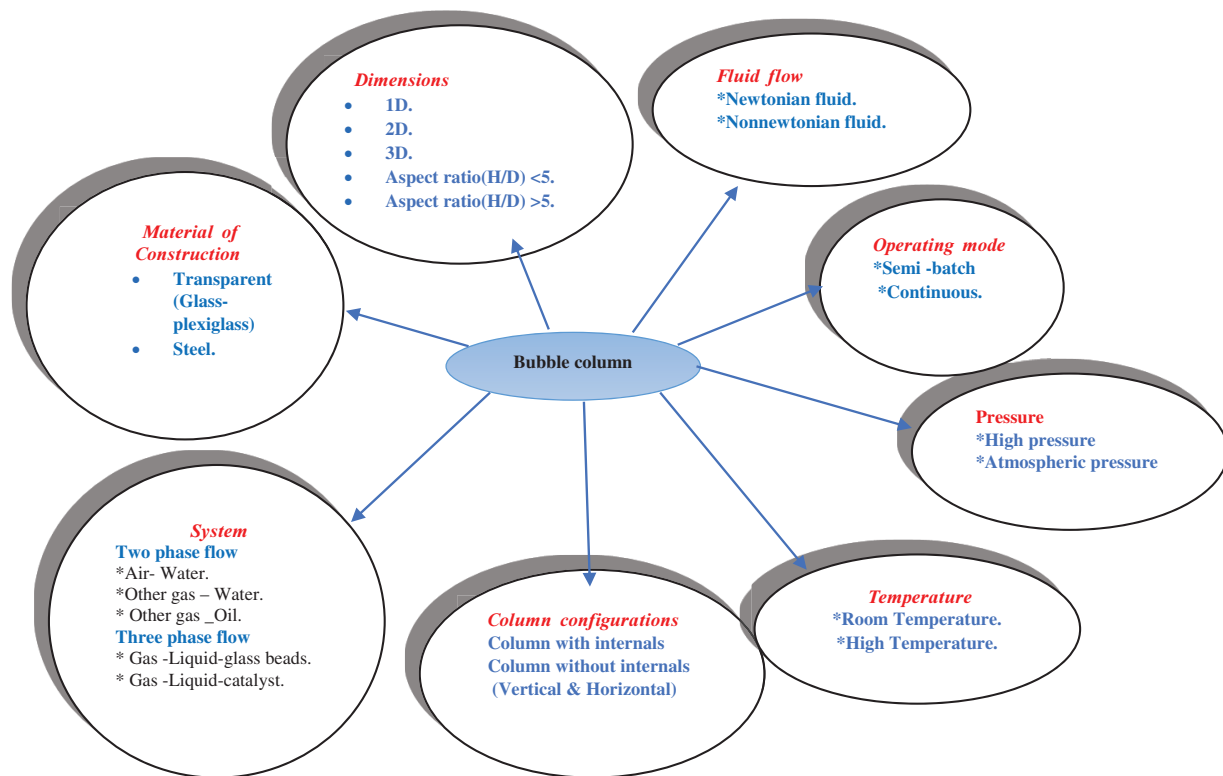


Figure 4: Conditions of bubble column

B-Gas sparger (gas inertia)

The gas sparger is the main component of the bubble column configuration. It is required for introducing gases into columns and has different designs and hole sizes. Moreover, it affects ε_G . The shape of the gas distributor affects the dynamics of bubbles entering through holes and those entering the reactor (bubble column). It imposes its effects on merging and substitution. Therefore, when a large-diameter distributor is used, large bubbles are ejected. By contrast, when a small-diameter distributor is used, small bubbles are ejected. The low-rise speed of small bubbles ensures that the bubbles remain for an adequate time in the reactor for fusion and replacement, making the ε_G obtained when a small-diameter distributor is used higher than that when a large-diameter distributor is applied [41]. Transition velocity decreases with an

increase in hole size up to a certain hole size. A gas sparger with a small hole size and large resistance will lead to small initial bubble size and large gas holdup in the homogeneous and transition regimes. The large gas holdup contributes a high volumetric mass transfer coefficient, which is a desirable characteristic. However, the gas holdup exhibits an excess and a slump in the transition regime when the small initial bubble size was adopted. The gas holdup slump results in pressure fluctuation, back mixing, and liquid residence time which should be avoided. There were varied experiments data for illustrating this relationship between superficial gas velocity and gas holdup [22].

2.7 Effect of Liquid Properties

2.7.1 Viscous Media

Viscosity has a dual effect on the liquid in a flow system. Besagni et al. studied the double effect of viscosity and found that ε_G increased nonlinearly and continuously if the viscosity of the liquid (μ_L) = 5% = 1.01 mPa s and small bubbles were produced but decreased significantly if the liquid viscosity was increased [36]. When viscosity is low, ε_G increases with an increase in the curve. The homogeneous regime is stabilized at low viscosity (4.25 mPa s) by increasing the liquid viscosity. Previous research has shown that the beginning gas velocity of the vortical spiral flow reduces with increasing viscosity at high viscosity (7.68 mPa s) [53]. An increase in viscosity in general advances flow regime transition.

2.7.2 Active Compounds

Scanning previously reported studies revealed that ε_G can be increased by increasing the number of active compounds, such as ethanol and electrolytes, in reactors. This change may influence flow regimes [54].

2.7.3 Inorganic Compounds

Inorganic compounds and their concentrations have an essential relationship with ε_G . Specifically, high inorganic compound concentrations in reactors (bubble columns) lead to significant increases in ε_G . Moreover, low inorganic compound concentrations lead to reductions in ε_G in bubble columns. A study using three electrolytes at different concentrations revealed that flow dynamics parameters increased with the increase in inorganic compound concentrations. Laboratory experiments on the effect of inorganic salts on ε_G and flow regimes in bubble columns are summarized in Table 2. A previous study using three salt solutions, namely, Solutions of Na_2SO_4 (p.a. grade), NaCl (p.a. grade), and NaCl (kitchen quality) were used, and it was found that the purity of the salt had a significant impact on the behavior of the bubble column and that some salts could have auxiliary effects that could skew results (such as crystallization inside plate orifices) [55].

2.7.4 Organic Compounds

Previous studies revealed that the addition of organic materials to flow systems in bubble column reactors cause foaming, which intensifies with the increase in the concentrations of organic compounds. Foam helps extend the residence time of gases in liquids and increase ε_G , thus enhancing system efficiency. However, these studies also showed that foam not only forms due to the increase in the concentrations of organic compounds, it is also affected by the ratio of the diameter of the reactor to its height and the location of gas entry. Ethanol is one of the most important organic compounds used in such systems [56,57].

2.8 Influence of Gas Properties

Gas and liquid properties influence the performance of bubble columns particularly in the presence of a real reaction. When using different types of gases, the size of gas bubbles varies from one gas to another due to differences in properties, such as pressure and temperature. This difference causes a variation in bubble size and distribution. For example, when the gas density (ρ_G) increases, ε_G increases, indicating that the

increase in ρ_G increases the residence time of the gas itself. Therefore, the use of the appropriate gas dispersion design should be considered to obtain the ideal operating condition of the system [58,59].

2.8.1 Pressure

Given that in general, liquid is an incompressible fluid, it is not influenced by pressure. Pressure does not have a noticeable effect on ε_G because it controls the operating conditions in the case of gas. However, its effect is slight. Pressure has a weaker effect on homogeneous flow than on heterogeneous flow and can be 6, 7, or 10 MPa depending on the operating conditions [48]. In general, an increase in pressure results in an increase in transition velocity.

2.8.2 Temperature

Some studies noted that increasing the temperature (T_c) does not affect flow dynamics parameters, such as ε_G . Meanwhile, Sato et al. [60] suggested that an inverse relationship exists between the temperature of the bubble column and ε_G . In general, increasing the temperature leads to the stage of evaporation, which helps release gas molecules to the surface quickly, resulting in a residence time that is insufficient for the completion of the reaction in the reactor. An increase in temperature increases the transition velocity and delays the flow regime transition.

2.8.3 Influence of Internals Hydrodynamics: “Holdup, Flow Regime”

Many times, bubble columns are investigated without taking internals into account (open tube bubble columns). However, in the majority of industrial applications, internal devices are frequently included to regulate heat transfer, promote bubble break-up, or prevent liquid phase back mixing. These components can significantly affect the multiphase flow inside the bubble column reactor, and it is still difficult to estimate these effects without doing experiments [61].

Table 2: Summary of the system properties of several literature studies reviewed for bubble columns reactor

Authors	System (gas/liquid)	Column diameter (m)	Column-gas distributor	Gas velocity (cm/s)	Dimension	Measurement	Conclusion
Abid et al. (2009) [62]	Air-water and air aqueous glycerin solutions	0.07, 0.15, 0.3	Perforated plate and ring type gas sparger	1–10	1 D	Delta function pulse	The flow regime transitions were examined using gas holdup measurements, and the local flow phenomena were examined using double fiber optical probes. Using the commercial program Ansys fluent.
Jawad (2009) [63]	Air water	0.2	Plexiglas with an entrance cone	4.5	1 D	The micro metering valve measurement	The two operating modes, batch and continuous, both used the axial dispersion model, whereas the continuous mode was the only one to use the tanks-in-series model.
Abid et al. (2010) [64]	Air water	0.45	Perforated plate	4.5–5	1 D	Two compressors connected in parallel, a pressure regulator and two rotameters	The results in the center of the column were 9%–13% higher than those close to the wall region because heat transfer coefficients rise with surface gas velocities.
Alwasiti et al. (2010) [65]	Air and non-Newtonian liquid of polyacrylamide	0.15	Perforated plate	/	1 D	Gas holdup for different concentrations of PAA	Using Newtonian and non-Newtonian liquids, this work compares the flow region in baffled and unbaffled bubble columns.
Alazzi et al. (2010) [66]	Air water	0.15	Average gas holdup	≤ 20	1 D	Using a gas meter, and two calibrated rotameters connected in parallel were used to measure the air flow rate	The impact of gas velocity, liquid-phase properties, solid-particle concentration, and static liquid height on both (G) and (K La). It has been found that (G) and (K La) rise with increasing gas velocity and fall with increasing concentrations of solid particles, static liquid height, viscosity, and liquid-phase surface tension.

(Continued)

Table 2 (continued)

Authors	System (gas/liquid)	Column diameter (m)	Column-gas distributor	Gas velocity (cm/s)	Dimension	Measurement	Conclusion
Walla'a Abdul Hadi Noori et al. (2012) [67]	Air water	0.075	Perforated plate	8, 12, 16	1 D	Using two calibrated rotameters	The current study investigated the absorption of carbon dioxide in a bubble column using a 0.5 M sodium hydroxide aqueous solution with and without varying concentrations of organic compounds, including glucose, fructose, and saccharose (0.05, 0.2, and 0.4 M), as well as varying superficial gas velocities (0.008, 0.012, and 0.016 m/s).
Alhaboubi et al. (2012) [68]	Air water	0.08	Porous distributor	16–27	1 D	Slurry reactor	In this paper, measurements of gas adsorption and ion-exchange were made using a bubble column slurry reactor.
Abdulrazzaq (2014) [69]	Air water	0.15–0.3	Bubble column reactors are preferred	8–200 and 8–30	1 D	Bed expansion technique	In gas-liquid systems (bubble columns), the effects of vertical cooling internals on the gas hydrodynamics were examined for column diameters of 15 and 30 cm in both the absence and presence of internals (the % occluded area by internals 5%, 10%, and 20%). The range of the surface gas velocity was changed.
Al-Naimi et al. (2019) [70]	Air-water	0.075	Perforated sparger	25	1 D	Using two separate calibrated rotameters.	The findings demonstrated that the dissolved gas experiences a pseudo-first order reaction, with $U_g = 0.025$ m/sec being the ideal surface gas velocity given a greater conversion and reaction rate.
Luo et al. (2011) [71]	Air–water	0.1	Perforateplate	2–12	2 D	The gamma-ray source (Cs-137, 100 mCi)	A change in flow regime can have a major impact on the performance of the bubble column. Since the current flow regime has an impact on mass and heat transfer as well as mixing in a reactor,
Liu et al. (2014) [72]	Air–water	0.1016	The distributor with 70 holes of 2 mm	12	2 D	Model (CFD–PBM) implemented in the open source CFD	Both the k-model and RSM make accurate predictions about the gas holdup.
Pourtousi et al. (2015) [73]	Air–water	0.288	single sparger with 20 holes	15–25	1 D	The eulerian–method to numerically	In addition to the ANFIS approach, this study uses CFD to simulate bubble column hydrodynamics for the homogeneous regime.
Besagni et al. (2017) [49]	Air-water-monoethylene glycol solutions	0.24	orifice sparger	4–20	3 D	An image analysis method	Because of the reduced/promoted coalescence phenomenon, a change in the liquid phase properties impacts the bubble interfacial properties at the “bubble-scale,” changing the prevalent bubble size distribution.
Maximiano Raimundo et al. (2016) [74]	Gas holdup and liquid velocity	0.15–3	The gas distributors are perforated plates	6–35	1 D	Coupled with others concerning gas holdup and axial liquid velocity	To create an experimental database that will help future modeling efforts and clarify scale-up criteria, size measurements have been combined with those pertaining to gas holdup and axial liquid velocity. At every scale, the average bubble diameters have been shown to be similar globally.
Fard et al. (2017) [75]	Gas-water–propanol (alcohol)	0.1	Sparger	6	1 D	Experimental measurements of the local hold-up and liquid velocity	Based on the authors' prior experiences, the physical models for the momentum transfer between phases—including drag, lift, and wall force—were selected.
Besagni et al. (2016) [61]	Air water	0.15	Sparger 7 downward facing orifice	3–35	1 D	Fast response heat flux probe, pressure transducers	In the open tube and annular gap designs, we conduct an experimental analysis of a counter-current gas-liquid bubble column. Two vertical internal tubes in the annular gap bubble column are taken into consideration.
Kagumba et al. (2015) [76]	Air water	0.14	Perforated plate 121 holes	3–45	1 D	Four Point optical probe	The purpose of this study is to investigate the effects of arrangements of dense internals with different diameters across the same cross-sectional area on the bubble dynamics, including local and global gas hold-up, a specific interfacial area, and axial bubble velocity.

(Continued)

Table 2 (continued)

Authors	System (gas/liquid)	Column diameter (m)	Column-gas distributor	Gas velocity (cm/s)	Dimension	Measurement	Conclusion
Al Mesfer et al. (2016) [77]	Air water	0.14	Perforated plate 121 holes	5	3 D	Y-ray Computed Tomography	Because when the velocity is estimated using the total cross-sectional area of the column, incorporating the internals causes a significant increase in both the global and local gas holdup. The gas holdup distribution over the cross-sectional area (CSA) of the column in the presence of internals has a symmetrical form at low gas velocities and an asymmetrical shape at higher ones for the honeycomb arrangement and its installation used in this work.
Al Mesfer et al. (2017) [78]	Air water	0.152	Perforated plate 121 holes	5	3 D	Y-ray Computed Tomography	The studies' findings show that a rise in superficial gas velocity in the presence of internals generates an increase in axial centerline liquid velocity and a dramatic drop in turbulence parameters, while a decrease in superficial gas velocity without internals causes an increase in both.
Kalaga et al. (2017) [79]	Air water	0.17	Perforated plate 30 holes	14–26.5	1 D	Radioactive particle tracking	The arrangement of the heat exchanger internals, surface gas, and liquid velocities have a significant impact on the liquid phase hydrodynamics and mixing characteristics, according to the results of this study.
George et al. (2017) [80]	Air water	0.15	Sparger 7 downward facing orifice	3–30	1 D	Camera, conductivity probes, fast response heat flux probe	Measurements with a fast response heat flux probe in two and three phase systems are compared and analyses to demonstrate its potential use for screening of internals
Sultan et al. (2018) [81]	Air water	0.14	Perforated plate 121 holes	5–45	2 D	Y-ray Computed Tomography	In all the tested designs, the inclusion of vertical tubes resulted in an increase in the gas holdup values at the bubble column's wall region. With the hexagonal design, the gas holdup values did experience a striking boost.
Taofeeq et al. (2018) [82]	Air water	0.14	Porous sheet	14–25	1 D	Fast response heat transfer probe, optical fiber probe	that because of the direct relationship between the local heat transfer coefficient and the local gas hydrodynamics, the submerged heat exchanger tubes improved heat transmission by boosting local gas holdup and bubble frequency.
Nedeltche et al. (2018) [83]	Air water	0.1	Wire Mesh sensors	1–15	1 D	Wire Mesh sensors	A superficial gas velocity (U_G) of 0.06 m/s marked the beginning of the homogeneous regime's first transition velocity Utrans-1 and the conclusion of the heterogeneous regime's second transition velocity Utrans-2. The revised parameters showed clear minima at these crucial velocities.
Möller et al. (2018) [84]	Air water	0.1	Perforated plate	2–14	1 D	Ultrafast X-ray computed tomography	According to the analysis of the gas holdup data across the whole cross-section of the column, the Utrans-1 and Utrans-2 values occurred at slightly lower UG values (0.05 and 0.08 m/s). These essential gas velocities controlled the lower and upper bounds of the transition regime.
Manjrekar et al. (2019) [85]	Air water	0.45	Perforated plate	20–40	2 D	Optical probe technique	In the current work, data from optical probe technology and machine learning are used to create a data driving model for identifying the flow regime in bubble column.
Xu et al. (2020) [86]	Gas-liquid	0.18	Perforated plate	3–35	1 D	The differential pressure transmitters	When the fractal dimension of bubbles rises from 0.56 to 2.56, the gas holdup and volumetric mass transfer coefficient increase by 120% and 42%, respectively.
Guan et al. (2021) [87]	Air-water	0.15	Perforated plate	0–25	1 D	The differential pressure transmitters	These approaches provide varied values for the initial transitional surface gas velocity as internals-covered cross-sectional area (CSA) increases.
Gong et al. (2022) [22]	Air-water	0.28	Perforated plate	1–13	1 D	The differential pressure transmitters	Experimental results show that Small initial bubble size will lead to higher gas holdup and slump trend. To overcome the trade-off between sufficient gas holdup and slump trend.

That the global column hydrodynamic is not significantly affected by the presence of internals. Most industrial multiphase reactors use internal structures for heat transfer from/to the system, for controlling the flow structures, and for back mixing in the column. The presence of the internals stabilizes the homogeneous flow regime in terms of transition gas velocity and transition holdup value [61].

All interior components, including perforated plates, baffles, vibrating helical springs, mixers, and heat exchanger tubes, are referred to as “internals” in this context. Instrumentation probes, downcomers, and risers with heat exchangers are all regarded as different types of internal barriers in commercial scale bubble columns.

Numerous studies have examined the properties of fluid dynamics locally or worldwide during the past few decades.

Studies on hydrodynamics parameters, particularly those related to flow regime hydrodynamics, are still rare. The distribution of G and bubble size should be studied, as shown in Table 2. Summary of the system properties of several literature studies reviewed for bubble columns reactor, in order to provide an ongoing multiscale assessment of bubble column fluid dynamics that takes into account the effects of heat and mass transfer.

Acknowledgement: The authors would like to thank the Missouri University of Science and Technology, the University of Technology-Iraq, and the Al Mustaqbal University College for financial support for this work. In addition, the authors would like to acknowledge the graduate student’s effort (Zahraa W. Hasan) in implementing the reviewer’s and the editor’s comments.

Funding Statement: The authors received no specific funding for this study.

Author Contributions: The authors confirm contribution to the paper as follows: study conception and design: Laith S. Sabri and Abbas J. Sultan; data collection: Ayat N. Mahmood; analysis and interpretation of results: Ayat N. Mahmood, Amer A. Abdulrahman, Hasan Shakir Majdi; draft manuscript preparation: Laith S. Sabri, Abbas J. Sultan and Muthanna H. Al-Dahhan. All authors reviewed the results and approved the final version of the manuscript.

Availability of Data and Materials: The data that support the findings of this study are available from the corresponding author, Laith S. Sabri, upon reasonable request.

Conflicts of Interest: The authors declare that they have no conflicts of interest to report regarding the present study.

References

1. Karn, A. (2017). Characterization of bubbly flow systems: A review. *International Journal of Petrochemical Science & Engineering*, 2(6), 286–290.
2. Yunos, M. A. S. M., Halim, N. K. A., Hussain, S. A., Yusoff, H. M., Sipaun, S. (2017). Investigations of bubble size, gas hold-up, and bubble rise velocity in quadrilateral bubble column using high-speed camera. *American Journal of Engineering, Technology and Society*, 4(1), 5–15. <http://www.openscienceonline.com/journal/archive2?journalId=737&paperId=3685>
3. Kulkarni, A. V., Joshi, J. B. (2011). Design and selection of sparger for bubble column reactor. Part I: Performance of different spargers. *Chemical Engineering Research and Design*, 89(10), 1972–1985. <https://doi.org/10.1016/j.cherd.2011.01.004>
4. Lau, R., Mo, R., Sim, W. S. B. (2010). Bubble characteristics in shallow bubble column reactors. *Chemical Engineering Research and Design*, 88(2), 197–203.
5. Millán-Núñez, R., Santamaría-del-Ángel, E., Cajal-Medrano, R., Barocio-León, Ó. A. (1999). El delta del Río Colorado : Un ecosistema con alta productividad primaria. *Ciencias Marinas*, 25(4), 509–524.

6. Mezui, Y., Cartellier, A., Obligado, M. (2023). An experimental study on the liquid phase properties of a bubble column operated in the homogeneous and in the heterogeneous regimes. *Chemical Engineering Science*, 268, 118381.
7. Taitel, Y., Barnea, D., Dukler, A. E. (1980). Modelling flow pattern transitions for steady upward gas-liquid flow in vertical tubes. *AIChE Journal*, 26(3), 345–354.
8. Kataoka, I., Ishii, M., Mishima, K. (1983). Generation and size distribution of droplet in annular two-phase flow. *Journal of Fluids Engineering*, 105(2), 230–238.
9. Jones Jr, O. C., Zuber, N. (1975). The interrelation between void fraction fluctuations and flow patterns in two-phase flow. *International Journal of Multiphase Flow*, 2(3), 273–306.
10. Merilo, M., Dechene, R. L., Cichowlas, W. M. (1977). Void fraction measurement with a rotating electric field conductance gauge. *Journal of Heat Transfer*, 99(2), 330–332.
11. Matsui, G. (1984). Identification of flow regimes in vertical gas-liquid two-phase flow using differential pressure fluctuations. *International Journal of Multiphase Flow*, 10(6), 711–719.
12. Barnea, D., Luninski, Y., Taitel, Y. (1983). Flow pattern in horizontal and vertical two phase flow in small diameter pipes. *The Canadian Journal of Chemical Engineering*, 61(5), 617–620.
13. Tapucu, A., Merilo, M. (1977). Studies on diversion cross-flow between two parallel channels communicating by a lateral slot. II: Axial pressure variations. *Nuclear Engineering and Design*, 42(2), 307–318.
14. Jones Jr, O. C., Delhaye, J. M. (1976). Transient and statistical measurement techniques for two-phase flows: A critical review. *International Journal of Multiphase Flow*, 3(2), 89–116.
15. Mi, Y., Ishii, M., Tsoukalas, L. H. (2001). Flow regime identification methodology with neural networks and two-phase flow models. *Nuclear Engineering and Design*, 204(1–3), 87–100.
16. Noraishah, O., Mohd, A. H., Ainul, M. T. (2011). The hydrodynamics studies of bubbling phenomena using high speed camera: A visual observation. *NTC 2011: Nuclear Technical Convention 2011*, Bangi, Malaysia.
17. Hooshyar, N. (2013). Hydrodynamics of structured slurry bubble columns. In: *Chemical engineering*. Iran: University of Tehran.
18. Buwa, V. V., Ranade, V. V. (2002). Dynamics of gas–liquid flow in a rectangular bubble column: Experiments and single/multi-group CFD simulations. *Chemical Engineering Science*, 57(22–23), 4715–4736.
19. Kawagoe, K. (1976). Flow-pattern and gas-holdup conditions in gas-sparged contactors. *International Chemical Engineering*, 16, 176–183.
20. Wu, B., Firouzi, M., Mitchell, T., Rufford, T. E., Leonardi, C. et al. (2017). A critical review of flow maps for gas-liquid flows in vertical pipes and annuli. *Chemical Engineering Journal*, 326, 350–377. <https://doi.org/10.1016/j.cej.2017.05.135>
21. Krishna, R., van Baten, J. M., Urseanu, M. I. (2000). Three-phase eulerian simulations of bubble column reac (Urseanu and Krishna, 2000). Tors operating in the churn-turbulent regime: A scale up strategy. *Chemical Engineering Science*, 55(16), 3275–3286.
22. Gong, C. K., Xu, X., Yang, Q. (2022). Gas holdup at dynamic equilibrium region of a bubble column: Effect of bubble generator performance. *Chemical Engineering Journal*, 443, 136382.
23. Behkish, A., Lemoine, R., Sehabiague, L., Oukaci, R., Morsi, B. I. (2007). Gas holdup and bubble size behavior in a large-scale slurry bubble column reactor operating with an organic liquid under elevated pressures and temperatures. *Chemical Engineering Journal*, 128(2–3), 69–84.
24. Youssef, A. A., Al-Dahhan, M. H., Dudukovic, M. P. (2013). Bubble columns with internals: A review. *International Journal of Chemical Reactor Engineering*, 11(1).
25. Jia, J., Babatunde, A., Wang, M. (2015). Void fractin measurement of gas-liquid two-phase flow from differential pressure. *Flow Measurement & Instrumentation*, 41, 75–80.
26. Rahim, E., Revellin, R., Thome, J., Bar-Cohen, A. (2011). Characterization and prediction of two-phase flow regimes in miniature tubes. *International Journal of Multiphase Flow*, 37(1), 12–23.
27. Hughmark, G. A. (1967). Holdup and mass transfer in bubble columns. *Industrial & Engineering Chemistry Process Design and Development*, 6(2), 218–220.

28. Mashelkar, R. A., Sharma, M. M. (1970). Mass transfer in bubble and packed bubble columns. *Transactions of the Institution of Chemical Engineers*, 48, T162–T162.
29. Akita, K., Yoshida, F. (1973). Gas holdup and volumetric mass transfer coefficient in bubble columns. Effects of liquid properties. *Industrial & Engineering Chemistry Process Design and Development*, 12(1), 76–80.
30. Hikita, H., Kikukawa, H. (1974). Liquid-phase mixing in bubble columns: Effect of liquid properties. *The Chemical Engineering Journal*, 8(3), 191–197.
31. O'Reilly, C. A., Chatman, J. (1986). Organizational commitment and psychological attachment: The effects of compliance, identification, and internalization on prosocial behavior. *Journal of Applied Psychology*, 71(3), 492.
32. Besagni, G., Guédon, G., Inzoli, F. (2014). Experimental investigation of counter current air-water flow in a large diameter vertical pipe with inners. *Journal of Physics: Conference Series*, 547, 12024.
33. Besagni, G., Guédon, G. R., Inzoli, F. (2016). Annular gap bubble column: Experimental investigation and computational fluid dynamics modeling. *Journal of Fluids Engineering*, 138(1), 011302.
34. Begovich, J. M., Watson, J. S. (1978). *Hydrodynamic characteristics of three-phase fluidized beds*, vol. 3, pp. 190–195. Cambridge: Cambridge University Press.
35. Catros, A., Bernard, J. R., Briens, C., Bergougnou, M. A. (1985). Gas holdup above the bed surface and grid gas jet hydrodynamics for three phase fluidized beds. *The Canadian Journal of Chemical Engineering*, 63(5), 754–759.
36. Fan, L. S., Bavarian, F. R., Gorowara, I., Kreischer, B. E. (1987). Hydrodynamics of gas-liquid-solid fluidization under high gas hold-up conditions. *Powder Technology*, 53, 285–29.
37. Song, G. H., Bavarian, F., Fan, L. S. (1989). Hydrodynamics of three-phase fluidized bed containing cylindrical hydrotreating catalysts. *Canadian Journal of Chemical Engineering*, 67, 265–275.
38. Gorowara, R. L., Fan, L. S. (1990). Effect of surfactants on three-phase fluidized bed hydrodynamics. *Industrial and Engineering Chemistry Research*, 29, 882–889.
39. Safoniuk, M., Grace, J. R., Hackman, L., McKnight, C. A. (1999). Use of dimensional similitude for scale-up of hydrodynamics in three-phase fluidized beds. *Chemical Engineering Science*, 54(21), 4961–4966.
40. Ramesh, K., Murugesan, T. (2002). Minimum fluidization velocity and gas holdup in gas-liquid-solid fluidized bed reactors. *Journal of Chemical Technology & Biotechnology*, 136, 129–136.
41. Kumar, R. N., Vinod, A. V. (2014). Oxygen mass transfer in bubble column bioreactor. *Periodica Polytechnica Chemical Engineering*, 58(1), 21–30.
42. Nacef, S., Poncinb, S., Bouguettouchaa, A., Wild, G. (2007). Drift flux concept in two- and three-phase reactors. *Chemical Engineering Science*, 62, 7530.
43. Jena, H. M., Sahoo, B. K., Roy, G. K., Meikap, B. C. (2008). Characterization of hydrodynamic properties of a gas-liquid-solid three-phase fluidized bed with regular shape spherical glass bead particles. *Chemical Engineering Journal*, 145(1), 50–56.
44. Abdel-aziz, M. H., El-abd, M. Z., Bassyouni, M. (2016). Heat and mass transfer in three phase fluidized bed containing high density particles at high gas velocities. *International Journal of Thermal Sciences*, 102, 145–153.
45. Rohini Kumar, P., Ramesh, K. V., Venkateswarlu, P. (2017). Phase holdups in a three-phase fluidized bed in the presence of coaxially placed string of spheres internal. *IOP Conference Series: Materials Science and Engineering*, 225, 012210.
46. Khalil, I. A., Kogure, K., Akita, H., Harashima, H. (2006). Uptake pathways and subsequent intracellular trafficking in nonviral gene delivery. *Pharmacological Reviews*, 58(1), 32–45.
47. Rollbusch, P., Bothe, M., Becker, M., Ludwig, M., Grünwald, M. et al. (2015). Bubble columns operated under industrially relevant conditions—current understanding of design parameters. *Chemical Engineering Science*, 126, 660–678.
48. Baawain, M. S., El-Din, M. G., Smith, D. W. (2007). Artificial neural networks modeling of ozone bubble columns: Mass transfer coefficient, gas hold-up, and bubble size. *Ozone: Science and Engineering*, 29(5), 343–352.

49. Besagni, G., Inzoli, F. (2017). The effect of liquid phase properties on bubble column fluid dynamics: Gas holdup, flow regime transition, bubble size distributions and shapes, interfacial areas and foaming phenomena. *Chemical Engineering Science*, 170, 270–296. <https://doi.org/10.1016/j.ces.2017.03.043>
50. Ding, R., Zhang, X., Chen, G., Wang, H., Kishor, R. et al. (2017). High-performance piezoelectric nanogenerators composed of formamidinium lead halide perovskite nanoparticles and poly (vinylidene fluoride). *Nano Energy*, 37, 126–135.
51. Laurent, S., Romain, L., Arsam, B., Yannick, H., Mariela, S. et al. (2008). Modeling and optimization of a large-scale slurry bubble column reactor for producing 10,000 bbl/day of fischer–tropsch liquid hydrocarbons. *Journal of the Chinese Institute of Chemical Engineers*, 39(2), 169–179.
52. Qiao, Z., Wang, Z., Zhang, C., Yuan, S., Zhu, Y. et al. (2012). PVAm–PIP/PS composite membrane with high performance for CO₂/N₂ separation. *AIChE Journal*, 59(4), 215–228.
53. Olivieri, G., Russo, M. E., Simeone, M., Marzocchella, A., Salatino, P. (2011). Effects of viscosity and relaxation time on the hydrodynamics of gas-liquid systems. *Chemical Engineering Science*, 66(14), 3392–3399. <https://doi.org/10.1016/j.ces.2011.01.027>
54. Pjontek, D., Parisien, V., Macchi, A. (2014). Bubble characteristics measured using a monofibre optical probe in a bubble column and freeboard region under high gas holdup conditions. *Chemical Engineering Science*, 111, 153–169. <https://doi.org/10.1016/j.ces.2014.02.024>
55. Zahradník, J., Fialova, M., Ru, M., Drahos, J., Kastanek, F. et al. (1997). Duality of the gas-liquid flow regimes in bubble column reactors. *Chemical Engineering Science*, 52(21–22), 3811–3826.
56. Besagni, G., Mereu, R., di Leo, G., Inzoli, F. (2015). A study of working fluids for heat driven ejector refrigeration using lumped parameter models. *International Journal of Refrigeration*, 58, 154–171.
57. Hur, Y. G., Yang, J. H., Jung, H., Lee, K. Y. (2014). Continuous alcohol addition in vaporized form and its effect on bubble behavior in a bubble column. *Chemical Engineering Research and Design*, 92(5), 804–811. <https://doi.org/10.1016/j.cherd.2013.08.006>
58. Besagni, G., Gallazzini, L., Inzoli, F. (2018). Effect of gas sparger design on bubble column hydrodynamics using pure and binary liquid phases. *Chemical Engineering Science*, 176, 116–126. <https://doi.org/10.1016/j.ces.2017.10.036>
59. Besagni, G., Inzoli, F., De Guido, G., Pellegrini, L. A. (2017). The dual effect of viscosity on bubble column hydrodynamics. *Chemical Engineering Science*, 158, 509–538. <https://doi.org/10.1016/j.ces.2016.11.003>
60. Sato, Y., Hirose, T., Takahashi, F., Toda, M. (1973). Pressure loss and liquid holdup in packed bed reactor with cocurrent gas-liquid down flow. *Journal of Chemical Engineering of Japan*, 6(2), 147–152.
61. Al Mesfer, M. K., Sultan, A. J., Al-Dahhan, M. H. (2016). Impacts of dense heat exchanging internals on gas holdup cross-sectional distributions and profiles of bubble column using gamma ray computed tomography (CT) for FT synthesis. *Chemical Engineering Journal*, 300, 317–333.
62. Abid, M. F., Jameel, F. S. (2009). Scale effects on the hydrodynamics of bubble column. *Engineering and Technology Journal*, 27(10), 1–23.
63. Jawad, A. H. (2009). Studies pressure drop of gas-non-newtonian liquid two phase flow in bubble column. *Engineering and Technology Journal*, 27(7), 1–15.
64. Abid, B. A., Abdulmohsin, R. S. (2010). Heat transfer characteristics in a large-scale bubble column operating in a semi-batch mod. *Engineering and Technology Journal*, 28(3), 562–578.
65. Alwasiti, A. A., Alsudany, F. T., Raad, A. (2010). Effect of baffles on homogenous-heterogeneous regime in two phase bubble column with non-newtonian liquid. *Engineering and Technology Journal*, 28(24), 6954–6969.
66. Alazzi, A. A. R. N. J. (2010). Gas hold-up and volumetric liquid-phase mass transfer coefficient in solid-suspended bubble columns with draught tube. *Engineering and Technology Journal*, 28(7), 1464–1483.
67. Muslem, M. A. (2012). Enhancement of carbon dioxide absorption in caustic soda by organic solutes addition. *Engineering and Technology Journal*, 30(15), 1–21.
68. Alhaboubi, N., Nori, N., Hamad, M. F. (2012). Chlorine removal with activated carbon using bubble column. *Engineering and Tech Journal*, 30(9), 15–37.

69. Abdulrazzaq, B. S. (2014). Fluid dynamic in bubble columns with heat exchanger internals. *Engineering and Technology Journal*, 32(11), 1–15.
70. Al-Naimi, S., Jasim, F., Kokaz, A. (2019). Dynamic study of carbon dioxide absorption using promoted absorbent in bubble column reactor. *Engineering and Technology Journal*, 37(1C), 70–78.
71. Luo, H. P., Al-Dahhan, M. H. (2011). Verification and validation of CFD simulations for local flow dynamics in a draft tube airlift bioreactor. *Chemical Engineering Science*, 66(5), 907–923.
72. Liu, Y., Hinrichsen, O. (2014). Study on CFD–PBM turbulence closures based on k – ϵ and reynolds stress models for heterogeneous bubble column flows. *Computers & Fluids*, 105, 91–100.
73. Pourtousi, M., Sahu, J. N., Ganesan, P., Shamshirband, S., Redzwan, G. (2015). A combination of computational fluid dynamics (CFD) and adaptive neuro-fuzzy system (ANFIS) for prediction of the bubble column hydrodynamics. *Powder Technology*, 274, 466–481.
74. Maximiano Raimundo, P., Cloupet, A., Cartellier, A. H., Beneventi, D., Augier, F. (2018). Hydrodynamics and scale-up of bubble columns in the heterogeneous regime: Comparison of bubble size, gas holdup and liquid velocity measured in 4 bubble columns from 0.15 m to 3 m in diameter. *Chemical Engineering Science*, 198, 52–61. <https://doi.org/10.1016/j.ces.2018.04.043>
75. Fard, M. G., Stiriba, Y., Gourich, B., Vial, C., Grau, F. X. (2020). Euler-euler large eddy simulations of the gas–liquid flow in a cylindrical bubble column. *Nuclear Engineering and Design*, 369, 110823.
76. Kagumba, M., Al-Dahhan, M. H. (2015). Impact of internals size and configuration on bubble dynamics in bubble columns for alternative clean fuels production. *Industrial & Engineering Chemistry Research*, 54(4), 1359–1372.
77. Sabri, L. S., Sultan, A. J., Majdi, H. S., Jebur, S. K., Al-Dahhan, M. H. (2022). A detailed hydrodynamic study of the split-plate airlift reactor by using non-invasive gamma-ray techniques. *ChemEngineering*, 6(1), 18. <https://doi.org/10.3390/chemengineering6010018>
78. Al Mesfer, M. K., Sultan, A. J., Al-Dahhan, M. H. (2017). Study the effect of dense internals on the liquid velocity field and turbulent parameters in bubble column for fischer–tropsch (FT) synthesis by using radioactive particle tracking (RPT) technique. *Chemical Engineering Science*, 161, 228–248.
79. Kalaga, D. V., Yadav, A., Goswami, S., Bhusare, V., Pant, H. J. et al. (2017). Comparative analysis of liquid hydrodynamics in a co-current flow-through bubble column with densely packed internals via radiotracing and radioactive particle tracking (RPT). *Chemical Engineering Science*, 170, 332–346.
80. George, K. J. H., Jhavar, A. K., Prakash, A. (2017). Investigations of flow structure and liquid mixing in bubble column equipped with selected internals. *Chemical Engineering Science*, 170, 297–305.
81. Sultan, A. J., Sabri, L. S., Al-Dahhan, M. H. (2018). Impact of heat-exchanging tube configurations on the gas holdup distribution in bubble columns using gamma-ray computed tomography. *International Journal of Multiphase Flow*, 106, 202–219.
82. Taofeeq, H., Al-Dahhan, M. (2018). Heat transfer and hydrodynamics in a gas-solid fluidized bed with vertical immersed internals. *International Journal of Heat and Mass Transfer*, 122, 229–251.
83. Nedeltchev, S., Möller, F., Hampel, U., Schubert, M. (2018). Flow regime transitions in a bubble column with internals based on a novel approach. *Journal of Chemical Engineering of Japan*, 51(4), 373–382.
84. Möller, F., Lau, Y. M., Seiler, T., Hampel, U., Schubert, M. (2018). A study on the influence of the tube layout on sub-channel hydrodynamics in a bubble column with internals. *Chemical Engineering Science*, 179, 265–283.
85. Manjrekar, O. N., Dudukovic, M. P. (2019). Identification of flow regime in a bubble column reactor with a combination of optical probe data and machine learning technique. *Chemical Engineering Science: X*, 2, 100023. <https://doi.org/10.1016/j.cesx.2019.100023>
86. Xu, X., Wang, J., Yang, Q., Wang, L., Lu, H. et al. (2020). Bubble size fractal dimension, gas holdup, and mass transfer in a bubble column with dual internals. *Chinese Journal of Chemical Engineering*, 28(12), 2968–2976.
87. Guan, X., Yang, N. (2021). Characterizing regime transitions in a bubble column with internals. *AIChE Journal*, 67(5), e17167.